Opto-Electronic Advances

Original Article

2018, Vol. 1, No. 6

DOI: 10.29026/oea.2018.180011

Probing defects in ZnO by persistent phosphorescence

Honggang Ye[1,2], Zhicheng Su[1], Fei Tang[1], Yitian Bao[1], Xiangzhou Lao[1], Guangde Chen[2], Jian Wang[1] and Shijie Xu[1]*

Native point defects in ZnO are so complicated that most of them are still debating issues, although they have been studied for decades. In this paper, we experimentally reveal two sub-components usually hidden in the low energy tail of the main broad green luminescence band peaking at 547 nm (~2.267 eV) in intentionally undoped ZnO single crystal by selecting the below-band-gap (BBG) optical excitations (e.g. light wavelengths of 385 nm and 450 nm). Moreover, both sub-components are manifested as long persistent phosphorescence once the BBG excitations are removed. With the aid of a newly developed model, the energy depths of two electron traps involved within the long lived orange luminescence are determined to be 44 meV and 300 meV, respectively. The candidates of these two electron traps are argued to be most likely hydrogen and zinc interstitials in ZnO.

Keywords: zinc oxide; defects; phosphorescence; photoluminescence

Ye H G, Su Z C, Tang F, Bao Y T, Lao X Z *et al*. Probing defects in ZnO by persistent phosphorescence. *Opto-Electronic Advances* **1**, 180011 (2018).

Introduction

Zinc oxide (ZnO) is a simple but outstanding inorganic compound having many applications in different fields such as catalysis, electro-acoustic transducers, transparent conductors, optoelectronics, paints & rubber, and pharmaceuticals etc.[1] These applications of ZnO often crucially depend on defects of this versatile material, especially for optoelectronics[2–5]. For example, a perfect and absolutely pure single crystal of ZnO would be an insulator rather than semiconductor at room temperature due to its wide bandgap of ~3.3 eV[6]. However, real single crystals of ZnO always exhibit n-type conductivity with electron concentrations varying over the whole range given for semiconductors (e.g. over 10 orders of magnitude)[1]. As pointed out by Hirschwald, such large variation in electron concentration is mainly caused by native point defects like interstitial zinc (Zn_i) and by shallow donor impurities (D), both located at 0.025–0.5 eV below the conduction band minimum[1]. Although theoretical and experimental studies have been extensively devoted to investigating the defects in ZnO[7–15], the nature and signatures of defects in ZnO still remains elusive. As an annotation of such situation, reliable p-type conductivity has not yet been realized in ZnO so far, despite considerable progresses in the field. It is thus essential to have a better understanding of defects in ZnO.

To elucidate so complicated problem of defects in ZnO, the proper choice of research-grade single crystals as the beginning sample could be a good idea[13,16–19]. On the other hand, recent development in more elaborate hybrid density functional theory calculation is also very helpful to update the understanding of defects in ZnO[20–22]. In addition, the discovery and modeling of visible phosphorescence in high-quality ZnO single crystal under the below-band-gap (BBG) optical excitations may pave a new way to investigate the defects in ZnO[19,23].

In this paper, we unveil the hidden orange and red sub-components of the common green luminescence (GL) band in an intentionally undoped ZnO single crystal grown with the melt-growth technique by taking BBG optical excitations. Both sub-components display long lived luminescence or phosphorescence behaviors after switching off the BBG excitations, while the GL band

[1]Department of Physics, and Shenzhen Institute of Research and Innovation (HKU-SIRI), The University of Hong Kong, Pokfulam Road, Hong Kong, China; [2]Department of Applied Physics, Xi'an Jiaotong University, Xi'an 710049, China

* Correspondence: S J Xu, E-mail: sjxu@hku.hk.

Received 24 May 2018; accepted 19 July 2018; accepted article preview online 24 July 2018

quickly quenches once the above-band-gap (ABG) excitation is removed. By examining the temperature evolution of the lifetimes of the orange phosphorescence component, we identify the two electron traps located at ~44 meV (D_1) and 300 meV (D_2), respectively, below the conduction band minimum of ZnO. The most possible candidates for D_1 and D_2 are argued to be hydrogen and zinc interstitials in ZnO, respectively.

Experimental

The sample used in this study was a high-quality ZnO single crystal in size of 10 mm×10 mm×0.5 mm (length × width × thickness) which was produced by Cermet Inc. It was grown with melt-growth method along the *c*-axis and polished on one face. In the variable-temperature photoluminescence (PL) experiments, the sample was mounted with silver paint on the cold finger of a Janis closed cycle cryostat providing a varying temperature range of 10 K–330 K. The excitation light sources used in the study were a 325 nm He-Cd laser (Kimmon), a light emitting diode (LED) with peak wavelength of 385 nm and full width at half maximum of 10 nm, and a laser diode with output wavelength of 450 nm. The PL signal dispersion and detection including time-resolved phosphorescence spectra were conducted on a home-assembled PL system composed of a monochromator with focus length of 300 mm (Acton SpectraPro 2300i) and a charge-coupled device (CCD) with 512 pixel×2048 pixel (Andor, Newton) as detector. Long-wavelength pass filters with cutting-edge wavelengths of 340 nm and 455 nm, respectively, were used to suppress residual excitation light. Time evolution of the phosphorescence signal from the sample after ceasing the BBG excitations was directly detected by a photomultiplier tube (PMT) (R928, Hamamatsu).

Results and discussion

Figure 1 illustrates a typical PL spectrum of the ZnO sample measured at 10 K under the excitation of a 325 nm He-Cd laser. Clearly, the overall PL spectrum consists of a sharp UV peak and a broad GL band centered at ~547 nm, which is well consistent with those commonly reported for high-quality ZnO in the literature. As shown by the inset in Fig. 1(a), the sharp UV peak is actually composed of a number of fine lines which have been well identified to be from free exciton (FX), donor-bound exciton (DX), and two-electron satellites (TES), as well as their longitudinal optical (LO) phonon sidebands[17,24–26]. The "valley" structure between FX-LO and DX-LO is caused by the many-body Fano resonance or interference[26]. Under the BBG excitations of 385 nm and 450 nm light, only visible emission bands are observed, as shown in Fig. 1(b). The visible emission excited by the 385 nm light was an orange luminescence (OL) band peaking at ~607 nm, while the orange and a highly structured red luminescence (RL) bands are simultaneously observed under the excitation of 450 nm light. This highly structured RL band has been identified as the $^4T_1(G)-{}^6A_1(S)$ internal transition of substitutional Fe^{3+} ion at Zn^{2+} site and its sidebands of different phonon models[27]. Notice that the three PL spectra in Fig. 1(b) are normalized for the sake of comparison. The actual intensities of the OL and RL bands are much weaker than that of the GL band. Justifying from some analogous and consistent local features, e.g., a few oscillatory structures near 650 nm in all the three visible PL spectra, one may conclude that both the OL and RL are actually the weak sub-components of the GL band.

Unlike the GL luminescence band, both the OL and RL bands can maintain for tens and hundreds of seconds after removing the BBG optical excitations. That is, they are manifested as typical long persistent phosphorescence (LPP) once the optical excitations are removed. However, the GL band decays so rapidly that it becomes unobservable once the ABG excitation is stopped. Therefore, the LPP phenomenon of the visible emissions in ZnO is somehow dissimilar with the persistent photoconductance in ZnO which can be observed for both ABG and BBG optical excitations[28–31]. Even for the persistent photoconductance in ZnO, its mechanism has not yet been unified[32,33].

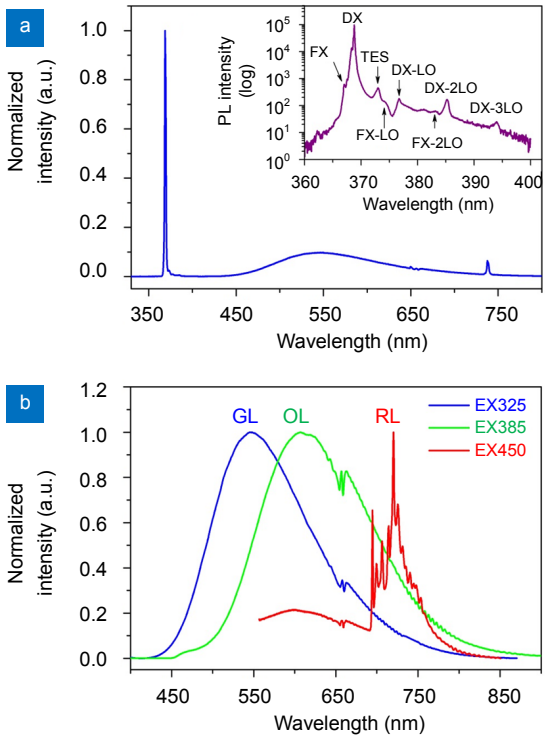

Fig. 1 | (Colour on-line) PL spectra of the ZnO bulk crystal at 10 K. (**a**) Full-range spectrum under the excitation of a 325 nm He-Cd laser. The inset reveals the detailed components of the sharp UV peak, including the principal lines of free exciton (FX), donor-bound exciton (DX) and two-electron satellites (TES), as well as their longitudinal optical (LO) phonon sidebands. (**b**) Defects induced visible emissions of the sample for the excitation wavelengths of 325 nm, 385 nm, and 450 nm.

Plotted in semi-logarithmic scale in Figs. 2(a) and 2(b) are the measured decay traces of the overall luminescence signal (directly monitored with a R928 PMT detector) of the sample at different temperatures after ceasing the 385 nm light excitation. All the decay traces were measured under the identical conditions except the variation of temperature so that the instantaneous intensities can be directly compared. As seen in Figs. 2(a) and 2(b), the measured decay traces of the OL phosphorescence do not follow a single exponential process at any temperature. In other words, none of the curves of Fig. 2(a) and 2(b) can be fitted with a single exponential decay function. However, each decay curve may be viewed as two segments. Previously, the similar non-single-exponential decay behaviors were observed for the copper-related structured GL band in ZnO after switching off the BBG optical excitation[19,23]. In thermochemically reduced MgO crystals, Jeffries *et al.* reported that the 2.3 eV phosphorescence of F centers exhibits similar attenuation in intensity once the BBG exciting light is withdrawn[34]. Nevertheless, they did not give explanations to such non-single-exponential decay behavior. But they found the first evidence for the main role of hydrogen as electron traps responsible for the long lived phosphorescence in MgO. Note that the overall OL phosphorescence intensity increases with the rise of temperature in the moderate high temperature range. When the temperature is increased beyond 150 K, the phosphorescence intensity turns to decrease with increasing the temperature, and finally vanishes at about 220 K. To examine time evolution of luminescence spectrum, we employed a home-assembled optical spectroscopy/imaging system comprised of monochromator + CCD detector to record time-resolved luminescence images of the sample at different temperatures after withdrawing the 385 nm excitation light. Two (taken at 50 K and 150 K) of the recorded phosphorescence images are illustrated in Figs. 2(c) and 2(d), respectively. From the images, it can be clearly seen that the lifetime of the OL band is much shorter than that of the RL band.

According to the conventional trapping-detrapping model, the LPP phenomenon in solids is interpreted as the slow charge transfer process from charge traps to luminescence centers[35]. However, the traditional model fails to give a quantitative explanation to the non-single-exponential decay behaviors of the phosphorescence signals observed in the nonintentional n-type ZnO and GaN crystals. To overcome this difficulty, we proposed an improved model taking into account both contributions of trapped electrons and free conduction-band electrons[23]. The new model may be represented as an analytic formula[23]:

$$I(t) \propto \left\{1+\frac{M}{[1-F\exp(-\gamma t)]^2}\right\}\exp(-\gamma t) \quad , \qquad (1)$$

where γ is the release probability of trapped electrons from trapping centers and its relationship with lifetime is $\gamma = 1/\tau$. From the γ values obtained by fitting the experimental decaying curves at different temperatures with eq. (1), one may obtain energy depth ΔE of a trap through employing a simple relationship, e.g. $\gamma(T) \propto \exp(-\Delta E / k_B T)$, where k_B is the Boltzmann constant. Doing so to the experimental decay curves shown in Figs. 2(a) and 2(b), two electron traps (e.g. D_1 and D_2) in the gap are determined to be 44 meV and 300 meV below the conduction-band minimum of ZnO, respectively, for the OL phosphorescence.

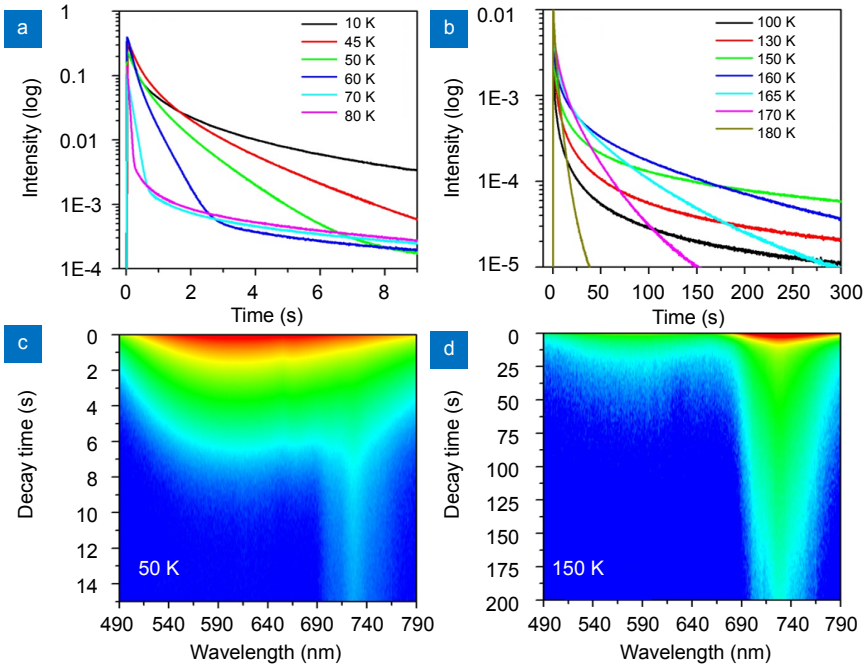

Fig. 2 | (**a**, **b**) (Colour on-line) Decaying traces of the visible luminescence of the sample at different temperatures after ceasing the 385 nm excitation. (**c**, **d**) show the recorded time-resolved phosphorescence images at 50 and 150 K, respectively.

Before we argue what are these two electron traps, it is important to recall the fact that physics and chemistry of defects even in high-quality intentionally undoped ZnO single crystal is very complicated, despite the simple chemical formula of ZnO. This is because wurtzite ZnO has a relatively open structure where Zn atoms occupy half of the tetrahedral sites and all the octahedral sites are empty. Such lattice stacking structure offers plenty of sites to accommodate intrinsic defects (e.g. Zn_i) and extrinsic impurities. Possible native point defects in ZnO, including O interstitials (O_i), Zn_i, Zn vacancies (V_{Zn}), V_O, zinc antisites (Zn_O), and O_{Zn}, have been extensively computed by different groups with different methods[7,8,10–12,36,37]. On one hand, these theoretical studies provide extremely valuable information and even guide to more fined experiments on complicated defects in ZnO. On the other hand, substantially different results produced by different methods also make something confused. According to Sokol *et al*' s theoretical calculations with hybrid exchange-correlation density functionals[10], singly positively charged Zn_i is the main electron donor located at 0.29 eV below the bottom of conduction band of ZnO. The energy depth of D_2 electron trap determined in the present study is in good agreement with this theoretical result. However, Janotti and van de Walle pointed out that Zn_i defects have high formation energies in n-type ZnO and are unlikely to be stable on the basis of their theoretical results[8]. Despite this inconsistency between relevant theoretical calculations, we tentatively assign the D_2 trap with an energy depth of 300 meV to the interstitial zinc in ZnO. For the much shallower D_1 trap, it is most likely interstitial hydrogen. Being very different from its role in other semiconductors, hydrogens can act as efficient shallow donor in ZnO[38]. In fact, hydrogen commonly exists in ZnO[39, 40] and other oxides such as MgO[34]. Hofmann *et al*. experimentally found the strong evidence of hydrogen cause as a shallow donor in state-of-the-art, nominally undoped ZnO single crystals and determined the activation energy of 35±5 meV[39]. By analyzing the temperature dependence of high-resolution electron energy loss spectroscopy signal of hydrogen in ZnO, Qiu *et al*. yielded a donor level ionization energy of 25±5 meV[40]. It is obvious that the energy depth (~44 meV) of D_1 electron trap determined in the present study is reasonably consistent with the ionization energy of hydrogen in ZnO obtained by them.

The origin of GL band has been a subject of considerable interest and extensive discussion. In fact, there exist two types of green luminescence in ZnO. One is the structureless GL band, while the other is the structured GL band with periodic fine structures. For the structured GL, the Cu ions (unintentionally or intentionally doped) have been firmly demonstrated to be responsible for it[9,18,19,22,41,42]. However, for the structureless GL band, which could be the most often seen color emission in various ZnO, very scattered origins, e.g. from substitutional Cu to V_O and V_{Zn}, and even surface states, have been proposed for it[43–45]. However, recent experimental studies consistently indicate multiple origins for the green luminescence in ZnO[44,45]. Čížek *et al*. experimentally show that the green luminescence in ZnO consists of a band at 2.3 eV due to recombination of electrons of the conduction band by V_{Zn} acceptors coupled with hydrogen and a band at 2.47 eV related to V_O[44]. Prucnal *et al*. experimentally demonstrate that the green emission in ZnO comes from V_{Zn}-related deep acceptor and V_{Zn}-V_O di-vacancy clusters, which is accompanied by the radiative transition between the triplet and the ground singlet state with the excited singlet state located above the conduction-band minimum. Moreover, they identify that the Zn_i is a shallow donor in ZnO, being mainly responsible for the n-type conductivity of intentionally undoped ZnO[45]. Recently, we employed the research-grade ZnO single crystals (e.g. with visible emission intensity 4 orders of magnitude lower than that of the near-band-edge UV emission at low temperature) + ion-implantation technique + underdamped multimode Brownian oscillator model simulations to the visible emissions to determine the two pure electron transitions of 2.92 eV and 2.40 eV for the green + red luminescence band[13,16,18]. From these studies and combining with theoretical results, V_{Zn} is most likely the origin of this 2.92 eV pure electronic transition, while V_{Zn}-V_O di-vacancy complex shall be responsible for the 2.40 eV pure electronic transition.

For the electron trap of the persistent photoconductance in ZnO, Kang et al. suppose that the hydrogen-zinc vacancy defect complex (2H-V_{Zn}) may be the microscopic origin[33]. They also reveal that the light absorption of 2H-V_{Zn} leads to the metastable state, leaving the free electrons in the conduction band. Furthermore, they estimate the lifetime of photo-electrons to be ~20 s. In the present study, we suggest that the interstitial hydrogens act as one shallower electron trap for the long phosphorescence, while the interstitial zinc trap electrons as the second electron supplier of the phosphorescence in ZnO.

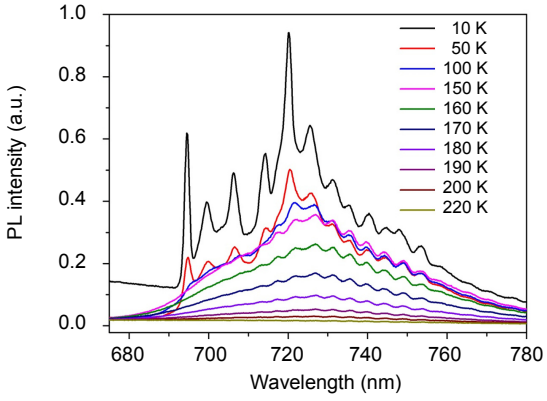

Fig. 3 | (Colour on-line) Variable-temperature PL spectra of the sample under the continuous excitation of 450 nm laser.

Finally, we briefly discuss the RL band. Thermal

quenching of the emission intensity and thermal smoothing of the sharp structures are simultaneously observed for the steady-state RL band of the sample under the BBG continuous excitation of 450 nm light, as shown in Fig. 3. Firstly, this luminescence band has been firmly identified by Heitz *et al.* as the $^4T_1(G)-{}^6A_1(S)$ internal transition of substitutional Fe^{3+} ion at Zn^{2+} site and its sidebands of different phonon models[27]. In addition, an optical excitation mechanism is suggested by these researchers in the study, which Fe^{3+} ion is excited by an indirect energy-transfer process from a deep acceptor to Fe^{2+} ion via capturing a photogenerated hole. In a recent study Zhou and his co-worker observed the evidence of electron trapping on Fe^{3+} ions in ZnO colloidal nanocrystals[46]. By investigating the correlation between electronic structure and magnetic properties of Fe-doped ZnO films, Chen *et al.* found that Fe^{2+} ions and localized defects like V_{Zn} play an important role for the ferromagnetism of the Fe-ZnO films, while Fe^{3+} ions at octahedral sites are dominant[47]. Considering the dominance of the RL band under the BBG excitation of 450 nm light as well as its long persistent phosphorescence behaviors, we propose an optical excitation and luminescence mechanism of Fe^{3+} ion in ZnO, which may be formulated as

$$\begin{aligned}
&\mathrm{Fe}_{\mathrm{Zn}}^{2+}+h\nu_{\mathrm{indigo}}\rightarrow\mathrm{Fe}_{\mathrm{Zn}}^{3+}+\mathrm{e}\,,\\
&\mathrm{e}+\mathrm{H}^{1+}\rightarrow\mathrm{H}+h\nu_{\mathrm{phonon}}\,,\\
&\mathrm{H}+\mathrm{Fe}_{\mathrm{Zn}}^{3+}+\mathrm{h}\rightarrow\mathrm{H}^{1-}+\mathrm{Fe}_{\mathrm{Zn}}^{3+}+h\nu_{\mathrm{phonon}}\,,\\
&\mathrm{Fe}_{\mathrm{Zn}}^{3+}\rightarrow\mathrm{Fe}_{\mathrm{Zn}}^{3+}+h\nu_{\mathrm{red}}+h\nu_{\mathrm{phonon}}\,. \qquad (2)
\end{aligned}$$

where $h\nu_{\mathrm{indigo}}$ and $h\nu_{\mathrm{red}}$ denote absorbed and emitted photons, respectively, $h\nu_{\mathrm{phonon}}$ means phonon (heat) generation, e and h imply electron and hole, respectively, H and Fe represent hydrogen and iron, respectively.

Conclusions

Defects induced visible luminescence of intentionally undoped n-type ZnO single crystal grown with melt-growth method was studied under the selected optical excitations of several wavelengths. It is found that the broad GL band contains two sub-components, e.g. an OL and a RL band in its low energy tail. Unlike the dominant component centered at 547 nm, both OL and RL sub-components exhibit long persistent phosphorescence for tens and even hundreds of seconds once the BBG optical excitations are removed. And phosphorescence lifetimes are found to be dependent distinctly on temperature. With the aid of a newly-developed phosphorescence model for time behaviors of phosphorescence in n-type wide bandgap semiconductors, the energy depths of involved electron traps are deduced to be 44 meV and 300 meV, respectively, in the bandgap of ZnO. Interstitial hydrogen and znic are argued to be the origins of two electron traps of 44 meV and 300 meV, while zinc vacancies and iron ions at zinc sites play essential roles in the GL-OL and RL luminescence in ZnO. These new findings shed some light on the defects and relevant visible emissions in ZnO, and are also of technological interest to ZnO community.

References

1. Hirschwald W H. Zinc oxide: an outstanding example of a binary compound semiconductor. *Acc Chem Res* **18**, 228–234 (1985).
2. Jagadish C, Pearton S J. *Zinc Oxide Bulk, Thin Films and Nanostructures*: *Processing, Properties, and Applications* (Elsevier, Amsterdam, 2006).
3. Klingshirn C F, Waag A, Hoffmann A, Geurts J. *Zinc Oxide*: *From Fundamental Properties Towards Novel Applications* (Springer, Berlin Heidelberg, 2010).
4. Sun X W, Yi Y. *ZnO Nanostructures and Their Applications* (CRC Press, New York, 2016).
5. Özgür Ü, Alivov Y I, Liu C, Teke A, Reshchikov M A *et al*. A comprehensive review of ZnO materials and devices. *J Appl Phys* **98**, 041301 (2005).
6. Srikant V, Clarke D R. On the optical band gap of zinc oxide. *J Appl Phys* **83**, 5447–5451 (1998).
7. Kohan A F, Ceder G, Morgan D, Van de Walle C G. First-principles study of native point defects in ZnO. *Phys Rev B* **61**, 15019–15027 (2000).
8. Zhang S B, Wei S H, Zunger A. Intrinsic n-type versus p-type doping asymmetry and the defect physics of ZnO. *Phys Rev B* **63**, 075205 (2001).
9. Shi S L, Li G Q, Xu S J, Zhao Y, Chen G H. Green luminescence band in ZnO: fine structures, electron−phonon coupling, and temperature effect. *J Phys Chem B* **110**, 10475–10478 (2006).
10. Sokol A A, French S A, Bromley S T, Catlow R A, Van Dam H J *et al*. Point defects in ZnO. *Faraday Discuss* **134**, 267–282 (2007).
11. Janotti A, Van de Walle C G. Native point defects in ZnO. *Phys Rev B* **76**, 165202 (2007).
12. McCluskey M D, Jokela S J. Defects in ZnO. *J Appl Phys* **106**, 071101 (2009).
13. Dai X M, Xu S J, Ling C C, Brauer G, Anwand W *et al*. Emission bands of nitrogen-implantation induced luminescent centers in ZnO crystals: experiment and theory. *J Appl Phys* **112**, 046102 (2012).
14. Fan J C, Sreekanth K M, Xie Z, Chang S L, Rao K V. P-type ZnO materials: theory, growth, properties and devices. *Prog Mater Sci* **58**, 874–985 (2013).
15. Bollmann J, Simon D K. Deep level defects in ZnO. *Physica B Condens Matter* **439**, 14–19 (2014).
16. Chen Y N, Xu S J, Zheng C C, Ning J Q, Ling F C C *et al*. Nature of red luminescence band in research-grade ZnO single crystals: a “self-activated” configurational transition. *Appl Phys Lett* **105**, 041912 (2014).
17. Ding L, Li B K, He H T, Ge W K, Wang J N *et al*. Classification of bound exciton complexes in bulk ZnO by magnetophotoluminescence spectroscopy. *J Appl Phys* **105**, 053511 (2009).
18. Chen Y N, Zheng C C, Ning J Q, Wang R X, Ling C C *et al*. Who make transparent ZnO colorful?–Ion implantation and thermal annealing effects. *Superlattices Microstruct* **99**, 208–213 (2016).
19. Ye H G, Su Z C, Tang F, Wang M Z, Chen G D *et al*. Excitation dependent phosphorous property and new model of the structured green luminescence in ZnO. *Sci Rep* **7**, 41460 (2017).
20. Alkauskas A, Pasquarello A. Band-edge problem in the theoretical determination of defect energy levels: the O vacancy in ZnO as a benchmark case. *Phys Rev B* **84**, 125206 (2011).

21. Koßmann J, Hättig C. Investigation of interstitial hydrogen and related defects in ZnO. *Phys Chem Chem Phys* **14**, 16392–16399 (2012).
22. Lyons J L, Alkauskas A, Janotti A, Van de Walle C G. Deep donor state of the copper acceptor as a source of green luminescence in ZnO. *Appl Phys Lett* **111**, 042101 (2017).
23. Ye H G, Su Z C, Tang F, Chen G D, Wang J *et al*. Role of free electrons in phosphorescence in n-type wide bandgap semiconductors. *Phys Chem Chem Phys* **19**, 30332–30338 (2017).
24. Rodnyi P A, Khodyuk I V. Optical and luminescence properties of zinc oxide (Review). *Opt Spectrosc* **111**, 776–785 (2011).
25. Wang X H, Xu S J. Two-electron-satellite transition of donor bound exciton in ZnO: radiative Auger effect. *Appl Phys Lett* **102**, 181909 (2013).
26. Xu S J, Xiong S J, Shi S L. Resonant coupling of bound excitons with LO phonons in ZnO: excitonic polaron states and Fano interference. *J Chem Phys* **123**, 221105 (2005).
27. Heitz R, Hoffmann A, Broser I. Fe^{3+} center in ZnO. *Phys Rev B* **45**, 8977–8988 (1992).
28. Melnick D A. Zinc oxide photoconduction, an oxygen adsorption process. *J Chem Phys* **26**, 1136–1146 (1957).
29. Takahashi Y, Kanamori M, Kondoh A, Minoura H, Ohya Y. Photoconductivity of ultrathin zinc oxide Films. *Jpn J Appl Phys* **33**, 6611–6615 (1994).
30. Murphy T E, Moazzami K, Phillips J D. Trap-related photoconductivity in ZnO epilayers. *J Electron Mater* **35**, 543–549 (2006).
31. Liao Z M, Lu Y, Xu J, Zhang J M, Yu D P. Temperature dependence of photoconductivity and persistent photoconductivity of single ZnO nanowires. *Appl Phys A* **95**, 363–366 (2009).
32. Lany S, Zunger A. Anion vacancies as a source of persistent photoconductivity in II-VI and chalcopyrite semiconductors. *Phys Rev B* **72**, 035215 (2005).
33. Kang Y, Nahm H H, Han S. Light-induced peroxide formation in ZnO: origin of persistent photoconductivity. *Sci Rep* **6**, 35148 (2016).
34. Jeffries B T, Gonzalez R, Chen Y, Summers G P. Luminescence in thermochemically reduced MgO: the role of hydrogen. *Phys Rev B* **25**, 2077–2080 (1982).
35. Li Y, Gecevicius M, Qiu J R. Long persistent phosphors—from fundamentals to applications. *Chem Soc Rev* **45**, 2090–2136 (2016).
36. Janotti A, Van de Walle C G. Fundamentals of zinc oxide as a semiconductor. *Rep Prog Phys* **72**, 126501 (2009).
37. Oba F, Choi M, Togo A, Tanaka I. Point defects in ZnO: an approach from first principles. *Sci Technol Adv Mater* **12**, 034302 (2011).
38. Van de Walle C G. Hydrogen as a cause of doping in Zinc Oxide. *Phys Rev Lett* **85**, 1012–1015 (2000).
39. Hofmann D M, Hofstaetter A, Leiter F, Zhou H J, Henecker F *et al*. Hydrogen: a relevant shallow donor in Zinc Oxide. *Phys Rev Lett* **88**, 045504 (2002).
40. Qiu H S, Meyer B, Wang Y M, Wöll C. Ionization energies of shallow donor states in ZnO created by reversible formation and depletion of H interstitials. *Phys Rev Lett* **101**, 236401 (2008).
41. Dingle R. Luminescent transitions associated with divalent copper impurities and the green emission from semiconducting Zinc Oxide. *Phys Rev Lett* **23**, 579–581 (1969).
42. Garces N Y, Wang L, Bai L, Giles N C, Halliburton L E. Role of copper in the green luminescence from ZnO crystals. *Appl Phys Lett* **81**, 622–624 (2002).
43. Ye J D, Gu S L, Qin F, Zhu S M, Liu S M *et al*. Correlation between green luminescence and morphology evolution of ZnO films. *Appl Phys A* **81**, 759–762 (2005).
44. Čížek J, Valenta J, Hruška P, Melikhova O, Procházka I *et al*. Origin of green luminescence in hydrothermally grown ZnO single crystals. *Appl Phys Lett* **106**, 251902 (2015).
45. Prucnal S, Wu J D, Berencén Y, Liedke M O, Wagner A *et al*. Engineering of optical and electrical properties of ZnO by non-equilibrium thermal processing: the role of zinc interstitials and zinc vacancies. *J Appl Phys* **122**, 035303 (2017).
46. Zhou D M, Kittilstved K R. Electron trapping on Fe^{3+} sites in photodoped ZnO colloidal nanocrystals. *Chem Commun* **52**, 9101–9104 (2016).
47. Chen T X, Cao L, Zhang W H, Zhang W, Han Y Y *et al*. Correlation between electronic structure and magnetic properties of Fe-doped ZnO films. *J Appl Phys* **111**, 123715 (2012).

Acknowledgements

This work was supported by a Hong Kong RGC-GRF Grant (Grant No. HKU 705812P), and National Natural Science Foundation of China (Grant No. 11374247, 11204231, 21373156).

Competing interests

The authors declare no competing financial interests.